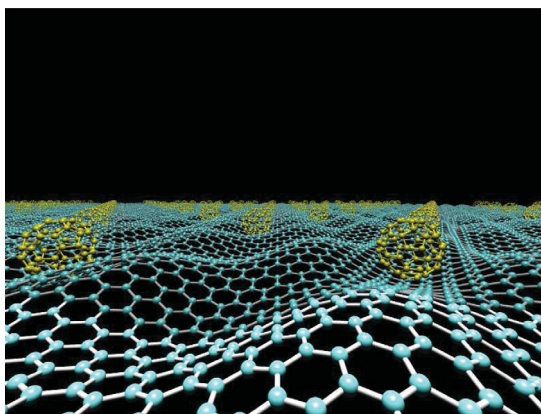


Molecular Self-Assembly on Graphene

J. M. MacLeod,* and F. Rosei*



From the Contents

1. Introduction.....1039
2. Molecule-Molecule and Molecule-Substrate Interactions in Molecular Self-Assembly.....1039
3. Self-Assembly of PTCDA, Phthalocyanines, and C₆₀ on Graphene.....1040
4. Exploring Graphene-Based Molecular Assemblies Through Other Molecules...1044
5. Emerging Applications of Graphene-Supported Molecular Layers.....1046
6. Conclusions and Outlook.....1046

The formation of ordered arrays of molecules via self-assembly is a rapid, scalable route towards the realization of nanoscale architectures with tailored properties. In recent years, graphene has emerged as an appealing substrate for molecular self-assembly in two dimensions. Here, the first five years of progress in supramolecular organization on graphene are reviewed. The self-assembly process can vary depending on the type of graphene employed: epitaxial graphene, grown in situ on a metal surface, and non-epitaxial graphene, transferred onto an arbitrary substrate, can have different effects on the final structure. On epitaxial graphene, the process is sensitive to the interaction between the graphene and the substrate on which it is grown. In the case of graphene that strongly interacts with its substrate, such as graphene/Ru(0001), the inhomogeneous adsorption landscape of the graphene moiré superlattice provides a unique opportunity for guiding molecular organization, since molecules experience spatially constrained diffusion and adsorption. On weaker-interacting epitaxial graphene films, and on non-epitaxial graphene transferred onto a host substrate, self-assembly leads to films similar to those obtained on graphite surfaces. The efficacy of a graphene layer for facilitating planar adsorption of aromatic molecules has been repeatedly demonstrated, indicating that it can be used to direct molecular adsorption, and therefore carrier transport, in a certain orientation, and suggesting that the use of transferred graphene may allow for predictable molecular self-assembly on a wide range of surfaces.

1. Introduction

The extraordinary properties of graphene^[1] have led to its intensive study since its isolation by mechanical cleaving of graphite in 2004.^[1a] One of the main technological accomplishments of this near-decade of intensive work has been the development of a variety of approaches for synthesizing graphene on surfaces. Many of these approaches are based on refining previously-identified procedures for forming epitaxial graphitic overlayers in ultrahigh vacuum (UHV), either from chemical vapour deposition onto clean single-crystal transition metals,^[2] or through carbon migration and/or decomposition, and have led to recipes for growing graphene on SiC,^[3,4] and on the (111)/(0001) hexagonal facets of a variety of metals, including Ni,^[5] Cu,^[6] Ru,^[7] Pd,^[8] Ir,^[9] and Pt.^[10] In addition, there are now also robust procedures for synthesizing high-quality epitaxial graphene outside of UHV,^[11] using a variety of carbon sources.^[12] Solution processing, which has the advantage of scalability, has been used to produce large films of graphene on Si/SiO₂.^[13] Novel processes can extend graphene growth to other non-reactive surfaces, including glass and plastic, at temperatures at or below 435 K.^[14] Tailoring the geometry of the graphene film is also possible, and specific attention has been given to developing methodologies for forming graphene ribbons^[15] and large-area graphene films,^[11,16] including progress towards wafer-scale graphene on SiC.^[17] A number of possibilities also exist for the transfer of graphene onto surfaces, which can be accomplished by solution deposition of exfoliated graphene or by transfer of epitaxial graphene; both of these options are now available commercially. This multiplicity of routes to the controlled synthesis of epitaxial and non-epitaxial graphene on a variety of surfaces makes it a versatile platform for device applications and materials design.

For a range of applications, the next step towards device integration will require modifying graphene for specific functionalities or electronic properties. Since graphene is natively a zero-bandgap semiconductor, its range of application can be expanded by introducing a bandgap through perturbations including confinement to nanoribbons, controlled introduction of strain, or biasing of bilayer graphene.^[18] Epitaxial graphene may possess an intrinsic doping due to its interaction with its substrate,^[19] and compensating for this offset may be required for applications. Covalent or noncovalent chemical functionalization^[20] can render normally-inert graphene chemically sensitive, which is critical for applications in sensing,^[21] and can allow for bandgap engineering/charge-transfer doping from electron donating/accepting organic molecules.^[22] The electronic effects produced by organic molecules on graphene have been either included in, or the focus of, a number of recent review papers.^[23]

On the other hand, graphene also presents an appealing testing ground for investigating the fundamental properties of molecular self-assembly confined to two dimensions. 2D supramolecular assembly is an active area of research geared toward understanding the energetics of supramolecular organization with the goal of establishing a predictive power over the controlled synthesis of useful 2D structures. In this context, graphene is a potentially useful new substrate that may

lead to new opportunities to control and extend the applications of surface-confined molecular structures. In this Review, we provide an overview of these last five years of work in molecular self-assembly on epitaxial graphene, with a focus on the influence of the graphene on molecular self-assembly.

2. Molecule-Molecule and Molecule-Substrate Interactions in Molecular Self-Assembly

Molecular self-assembly at surfaces depends critically on two types of interaction: molecule-substrate interactions that stabilize the molecules on the surface, and non-covalent molecule-molecule interactions that define the relationship between neighbouring molecules. A number of different intermolecular interactions can drive 2D self-assembly. Strong, directional bonds including coordination of metal centres^[24] and strong hydrogen bonds (e.g., carboxylic dimers^[25]) can produce porous assemblies.^[26] In general, weaker bonds, such as halogen-halogen^[27] and van der Waals interactions,^[28] produce a close-packed film where the areal molecular density is maximized. Mixing and matching of interactions allows for hierarchical control of assemblies,^[29] and for facilitation of multicomponent molecular architectures,^[30] including host-guest structures.^[31] A number of reviews are available to provide descriptions of molecular self-assembly from different perspectives.^[32] For all molecular films, but particularly for those with weaker intermolecular interactions that make the enthalpic contribution of the molecule-substrate interaction more important, the substrate plays a critical role, and preferred molecular adsorption sites define the growth of the film.

The adsorption of a number of different small aromatic molecules on isolated graphene has been investigated using density functional theory,^[33,34] and in general two attributes of the molecule-substrate interaction have emerged as common: (i) the molecules adsorb with their aromatic rings parallel to the surface, primarily stabilized by dispersive (van der Waals) interactions, and (ii) the lowest-energy adsorption geometry produces a “stacked” geometry where the molecular benzene rings follow the *AB* stacking of highly oriented pyrolytic graphite (HOPG).

Epitaxial graphene possesses unique attributes that can produce unique effects in graphene/molecular layer systems. Although graphene is usually described as a single layer of graphite, i.e. sp²-hybridized carbon bonded in-plane to three neighbours, both the structure and electronic properties of

Dr. J. M. MacLeod, Prof. F. Rosei
 Centre Énergie Matériaux Télécommunications
 Institut national de la recherche scientifique
 1650 Boul. Lionel-Boulet,
 Varennes, QC, J3X 1S2, Canada
 E-mail: macleod@emt.inrs.ca

Prof. F. Rosei
 Centre for Self-Assembled Molecular Structures
 801 Sherbrooke Street W.,
 Montreal, QC, H3A 2K6, Canada
 E-mail: rosei@emt.inrs.ca

DOI: 10.1002/sml.201301982



epitaxial graphene are dependent on the substrate on which it is grown, and can depart from the properties of isolated graphene.^[35] Superposition of the graphene and substrate lattices gives rise to an interference effect known as a moiré pattern, which defines a superlattice with a periodicity larger than either of the individual lattices. This superlattice creates both structural and electronic effects. The general considerations for moiré superlattice formation are described by Witterlin and Bocquet.^[36] The graphene-substrate electronic interaction is maximized when graphene C atoms are positioned over substrate atoms (top sites) and the corresponding reduced density of states near the Fermi level means that these regions in the moiré superlattice appear darker in scanning tunnelling microscopy (STM) images. These dark regions are further differentiated by whether the carbon atoms not positioned over top sites are located over *hcp* or *fcc* substrate hollow sites. Conversely, the bright regions of the moiré superlattice correspond to regions where the graphene C atoms sit above hollow sites (both *fcc* and *hcp*) in the underlying substrate. Spectral signatures of the electronic perturbation are evident in angle-resolved photoemission,^[37] and correspond in real space to a periodic structural and electronic modulation^[38] that creates a spatially-varying energetic landscape on the graphene.

Epitaxial graphene can be broadly divided into two classes: weakly interacting, where the Dirac-like dispersion of graphene is only slightly perturbed (e.g. on Ir(111) and SiC(0001)) and strongly interacting, where the spacing between substrate and graphene varies significantly over the moiré unit cell, and a bandgap of up to a few eV opens up at the \bar{K} point (e.g. Ru(0001) and Ni(111)).^[36a] This moiré landscape has been shown to direct the adsorption of metallic nanoclusters,^[38,39] and can have similar consequences for molecular adsorption (see below), especially at low temperature. However, when graphene interacts less strongly with its support it presents a much more HOPG-like adsorption landscape. For example, a detailed variable-temperature study of the diffusion and growth of 1,3,5-triazine on graphene/Pt(111) determined a diffusion barrier on graphene of 68 ± 9 eV as compared to 55 ± 8 eV for HOPG, indicating that diffusion on the two surfaces is unchanged within uncertainty.^[40] The cleanliness of the graphene also has a critical effect on molecular diffusion barriers. A combined transmission electron microscopy (TEM) and density functional theory (DFT) study showed that hydrogen adatoms on free-standing monolayer graphene can trap small molecules (OH, NH₂, CH₃) at the graphene surface, leading to a symbiotic stabilization of both the hydrogen impurity and the small molecule.^[41] However, as we describe below, most studies have focused on clean, well-formed systems where the energetics are dominated by molecule-molecule and molecule-substrate interactions, and not by defects.

3. Self-Assembly of PTCDA, Phthalocyanines, and C₆₀ on Graphene

To date, the majority of investigations of molecular self-assembly on graphene have focused on three molecules:



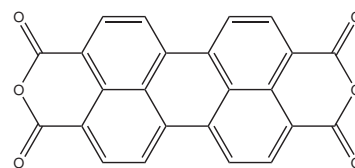
Jennifer MacLeod received her PhD in Physics from Queen's University (Kingston, Canada) in 2006. She subsequently held post-doctoral positions at INRS-EMT, working on scanning tunnelling microscopy studies of molecular self-assembly, and Università degli Studi di Trieste, where she made use of Elettra Synchrotron for materials characterization studies. In 2010 she returned to INRS-EMT, where she has continued her work on surface-confined molecular systems as a Research Associate. Dr. MacLeod is an author on over 30 papers in international peer-reviewed journals.



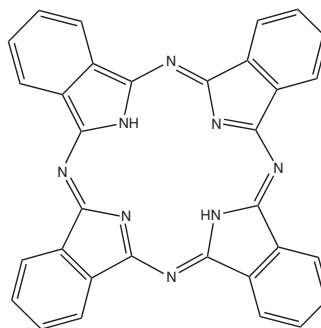
Federico Rosei holds the Canada Research Chair in Nanostructured Organic and Inorganic Materials, and is Professor and Director of the Energy, Materials and Telecommunications Centre of INRS in Varennes (QC) Canada. He obtained his PhD in 2001 from the University of Rome "La Sapienza" (Italy). He is Fellow of the American Association for the Advancement of Science, Fellow of the Royal Society of Chemistry (UK), Fellow of the Institute of Physics, Fellow of the Institution of Engineering and Technology, Fellow of the Institute of Materials, Metallurgy and Mining, Fellow of the

Institute of Nanotechnology, Senior Member of the IEEE, Fellow of the Engineering Institute of Canada, Member of the Global Young Academy, Fellow of the Australian Institute of Physics, Senior Member of SPIE and Member of the Sigma Xi Society.

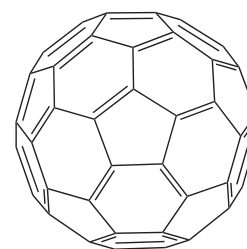
perylene-3,4,9,10-tetracarboxylic dianhydride (PTCDA), phthalocyanine (and its metal coordination complexes), and C₆₀ fullerenes (**Scheme 1**). Each of these molecules is a well-studied organic semiconductor whose structure is optimal for



PTCDA



PHALOCYANINE



C60 FULLERENE

Scheme 1. Molecular structures for PTCDA, phthalocyanine and C₆₀.

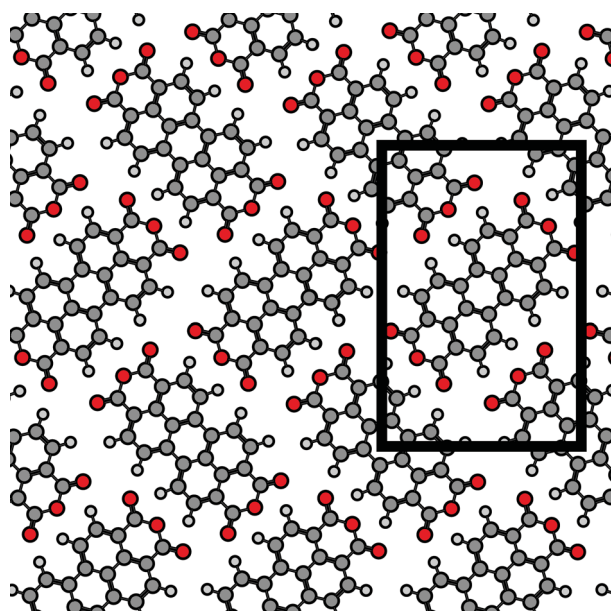


Figure 1. Schematic illustration of the PTCDA herringbone structure. A unit cell is outlined in black. The structure is stabilized by multiple C—H...O bonds.

π – π interactions with the underlying graphene.^[23] Investigations of their behavior on graphene have therefore combined studies of their adsorption and energetics with probes of the electronic modification introduced by their presence.

3.1. PTCDA

PTCDA, a prototypical polycyclic π -conjugated n-type organic semiconductor, has been extensively characterized on graphene surfaces because of its potential applications in organic graphene-based devices. In 2008, Lauffer and coworkers investigated the assembly of PTCDA on graphene bilayers on SiC(0001) using low temperature (LT) STM.^[42] They observed a “brick wall” structure at 4.7 K, wherein each molecule assumes an identical orientation, in contrast to the known structure formed by PTCDA on highly oriented pyrolytic graphite (HOPG), which is a herringbone structure comprising interlocking rows of planar-adsorbed PTCDA with alternating orientations,^[43] similar to both the (102) plane of the bulk structure^[44] and the structure formed on the (111) facet of Au, Ag and Cu^[45] (**Figure 1**). The brick wall structure observed on graphene is similar geometrically to the structure formed on Ag(110).^[45b] However, the higher molecular density on graphene led to the hypothesis that PTCDA might assume a non-planar adsorption geometry on graphene. Scanning tunneling spectroscopy (STS) data obtained from graphene neighboring the PTCDA assembly showed a 75 meV rigid shift, indicating electron transfer to the graphene sheet.

Room temperature investigations of PTCDA on monolayer graphene/SiC(0001) provide a more general picture of the characteristics of the assembly process. PTCDA forms into a well-organized herringbone structure (**Figure 2a**) in

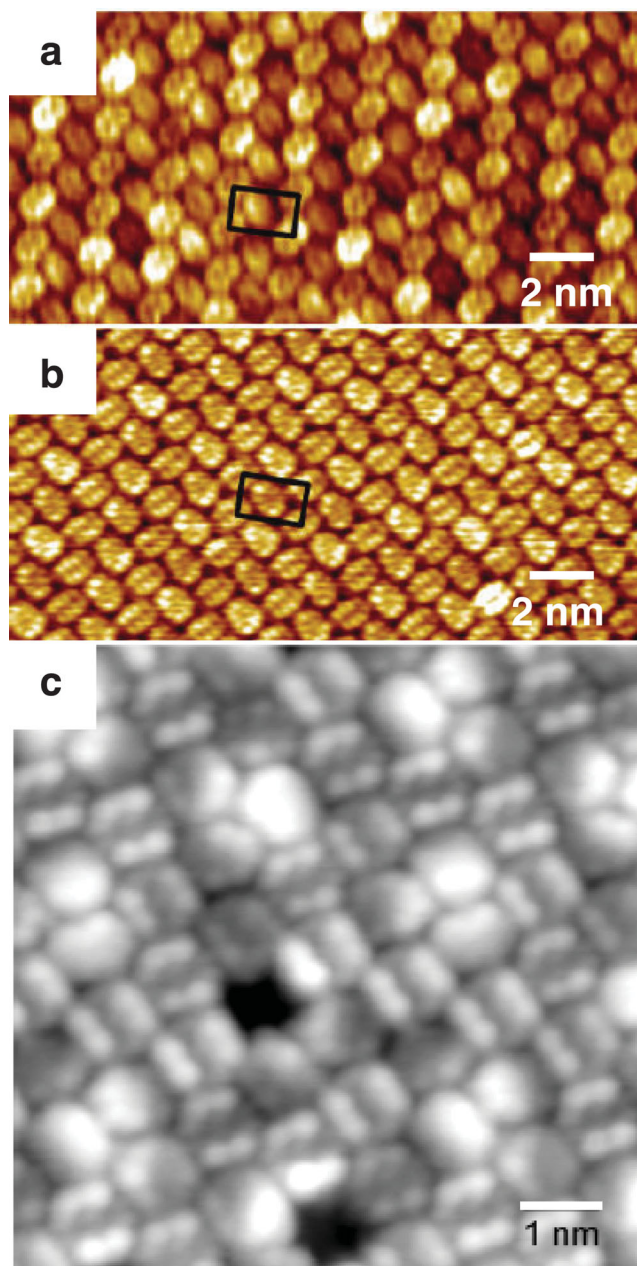


Figure 2. STM images showing the PTCDA herringbone structure on graphene/SiC(0001) (a), HOPG (b) and graphene/Ru(0001) (c). On graphene, the PTCDA exhibits a variation of contrast not observed on HOPG. The graphene/Ru(0001) structure images very bright with the periodicity of the moiré pattern and certain sites within the moiré pattern are prone to vacancy defects within the film. Tip bias voltages 2.5 V (a), 2.2 V (b) and 0.97 V (c). (a,b) Reproduced with permission.^[48] Copyright 2009, American Chemical Society. (c) Reproduced according to the Creative Commons license.^[50]

domains that extend hundreds of nanometers,^[46] crossing step edges in the underlying SiC and passing unperturbed over graphene defects including subsurface nanotubes and six-fold scattering centers; this robust behavior was later confirmed by a DFT-based *ab initio* calculations of the system.^[47] Submonolayer coverages produced isolated islands of the same structure.^[46] PTCDA on HOPG (Figure 2b) has an epitaxy matrix defined by PTCDA/HOPG interactions,^[43] and

exhibits 60° rotations between domains, consistent with STM/AFM observations of PTCDA/graphene,^[48] although some STM data suggest arbitrary orientations between domains.^[46] A comprehensive low-energy electron diffraction study on bilayer graphene/SiC(0001) confirms that the graphene and HOPG(0001) behave identically with respect to the epitaxial growth of PTCDA.^[49] STM images suggest that PTCDA grows in a layer-by-layer (Frank-van der Merwe) mode on epitaxial graphene/SiC(0001) for coverages up to ~3 ML,^[48] (the highest coverage used in the study) contrary to the *ab initio*-based prediction of Stranski-Krastanov growth with a critical thickness of 1 ML.^[47]

X-ray reflectivity data give the spacing between PTCDA and graphene as ~0.34 nm, which is close to the sum of the van der Waals radii and suggests that the layer is only weakly chemisorbed.^[51] STS spectra obtained from herringbone PTCDA on monolayer graphene/SiC(0001) at room temperature contain broad features attributable to the PTCDA lowest unoccupied molecular orbital (LUMO) at -1.1 eV and highest occupied molecular orbital (HOMO) at 1.8 eV.^[46] Spectra obtained at 77 K exhibit only two sharp features that were attributed to the PTCDA LUMO (-1.52 eV) and LUMO+1 (-1.78 eV); that the differences from the room temperature data may result from a temperature-dependence in the bonding geometry of PTCDA on graphene.^[48] X-ray photoelectron spectroscopy (XPS) measurements^[48] indicate a weak electron transfer from the graphene to PTCDA, as evidenced by a 0.25 ± 0.05 eV shift of the vacuum level following PTCDA deposition. The observed valence band spectra are consistent with bulk PTCDA, and core-level spectra reveal no binding energy shifts or new states, as expected for weak interaction between PTCDA and graphene. Differential reflectance measurements show a monomer-like reflectance for PTCDA in the first epitaxial layer, further confirming the minimal electronic interaction between PTCDA and graphene.^[49]

The growth of PTCDA on graphene/Ru(0001) demonstrates the importance of the graphene epitaxial structure in the epitaxy of aromatic molecules.^[50] The moiré pattern of graphene/Ru(0001) produces an extremely pronounced variation in the surface electronic structure, leading to a periodic variation in the observed adsorption potential for metallic clusters.^[39b] At both submonolayer and ML coverages, PTCDA on graphene/Ru(0001) forms islands or continuous films of the herringbone structure; however, the effect of the graphene moiré asserts itself in the prevalence of missing-molecule defects that occur on top of the bright sites in the graphene moiré pattern (Figure 2c). Using force field calculations, the difference in adsorption energy between the moiré dark and bright sites was found to be of the order of -0.4 to -0.7 eV.^[50] Density functional theory (DFT) calculations indicate that the hydrogen bond enthalpy per molecule is in the range of -0.4 to -0.6 eV for herringbone structures,^[52] suggesting that the energetics of the system are democratically determined by both the adsorption and the interaction energies.

3.2. Phthalocyanines

Phthalocyanines (shown as unsubstituted phthalocyanine, H₂Pc, in Scheme 1) can be employed as a sort of π -conjugated

organic cage for metal atoms coordinated at the centre of the structure; in this state, they are referred to as metal-phthalocyanines (M-Pc), and they have orbital energetics and spin states that are defined by the constituent metal centre and by any side groups. On HOPG, where they lie flat on the surface, van der Waals interactions between H-terminated M-Pc provide lateral stabilization to their self-assembled close-packed layers.^[53]

LT studies clearly elucidate the effect of the graphene substrate on M-Pc assembly. Following room temperature (RT) deposition and subsequent cooling to liquid-He temperature (~5 K) on graphene/Ru(0001), iron II Pc (FePc), nickel II Pc (NiPc) and H₂Pc each formed Kagome lattices with periodicities equal to the moiré periodicity, 3 nm.^[54] At lower coverages, FePc molecules selectively adsorb in the *fcc* valley regions of the moiré pattern.^[55] Following the saturation of the *fcc* valley sites, with increasing coverage, FePc preferentially adsorbs at the edge of the moiré sites, avoiding the *hcp* valley sites. Rather than depending on the site-specific binding energy, which would actually favor the *hcp* sites, the occupation of sites is determined by the strength of the lateral dipole induced in the graphene by its corrugation, which is greatest for *fcc* valley sites. The polarizability imparted by the metal atom in the FePc makes it an excellent candidate for dipole-driven site selection. Further, the authors demonstrate through observation of the preferred molecular adsorption sites at low coverage that different phthalocyanines interact differently with the graphene/Ru(0001) substrate, with interactions that order as FePc > MnPc > NiPc and H₂Pc.^[56] Under the same conditions on graphene/Pt(111), FePc assembles only into uniform close-packed islands or films, indicating no substrate effect.^[56]

At RT, and on lower-corrugation moiré patterns, the formation of a close-packed monolayer of flat-lying M-Pc is the dominant assembly motif, demonstrated by copper hexadecafluoro-phthalocyanine (F₁₆CuPc)/graphene/SiC(0001),^[57] FePc^[58] and CoPc^[59] on graphene/Ir(111), NiPc, CuPc, ZnPc, FePc and CoPc/graphene/Ni(111),^[60] for chloroaluminum phthalocyanine (ClAlPc) on graphene transferred onto ITO,^[61] and for CoPc/graphene/Si (both natively grown and transferred).^[62] The flat adsorption of the molecules was confirmed by near-edge x-ray absorption fine structure spectroscopy (NEXAFS) for both FePc/graphene/Ir(111)^[58a] and ClAlPc/graphene/ITO,^[61] by high-resolution electron energy loss spectroscopy for M-Pc/graphene/Ni(111),^[60] by x-ray diffraction and two dimensional grazing incidence X-ray scattering for CoPc/graphene/Si^[62] and by the flat or nearly-flat orientation evident in STM images.^[56–59,61,62] F₁₆CuPc/graphene/SiC(0001)^[57] and CoPc/graphene/Si^[62] exhibit preferential adsorption on monolayer graphene when bilayer graphene is also present at the surface, which in both cases can be attributed to a lower adsorption energy on the bilayer graphene (although this phenomenon is only evident at 400 K, and not RT, for CoPc/graphene/Si). After the completion of the first layer, the M-Pc molecules continue to lie flat or nearly flat in all systems for which molecular orientation in multilayers was measured.^[58a,60,62]

Many of the M-Pc molecules interact only weakly with the underlying graphene/substrate system: NEXAFS of FePc/

graphene/Ir(111) indicates that the empty states of the molecule are not modified by substrate interaction,^[58a] and a detailed photoemission study indicated that for the same system, a monolayer molecular coverage produced a 0.08 ± 0.02 eV shift of the Dirac cone towards higher binding energy, and a 0.25 eV increase in the work function.^[58b] A 10 nm film of CIAIPc on graphene/ITO produced a similar work function increase of 0.36 eV.^[54] For M-Pc on graphene/Ni(111), HREELS revealed stronger interactions for both FePc and CoPc, which couple to the graphene/Ni(111) through their metal ions, but show negligible changes to their aromatic structures.^[60] No interaction was detected for NiPc, CuPc and ZnPc, leading to the interpretation that the *d*-band filling of Fe and Co leave them likely to couple with the underlying Ni substrate, and that the interceding graphene layer is unable to prevent this interaction.

3.3. C₆₀

STM measurements of ML C₆₀ deposited onto graphene/Ru(0001) at 330 K and imaged at liquid He temperature reveal the formation of a close-packed layer of molecules that uniformly occupies all regions of the moiré mesh.^[63] The molecules within the layer are aligned with their hexagonal rings facing out and exhibit molecular orbitals that appear essentially unperturbed from their gas-phase structure. Further work, where C₆₀ was deposited at RT, annealed to 320 K and subsequently cooled to 50 K, showed that the C₆₀ structure is commensurate with the underlying graphene moiré pattern.^[64] However, incommensurate close-packed structures not aligned along the moiré superlattice were also formed, especially on surfaces where the graphene was defect-intensive due to incomplete annealing. The robust close-packing of the C₆₀ is attributed to the relatively strong intermolecular interactions, which are estimated to be −514 meV by DFT calculations, compared to substrate adsorption energies varying from −267 meV to −336 meV depending on the site within the moiré superlattice.

Following RT deposition and imaging, the behavior of the C₆₀ molecules is different. STM imaging of graphene/Ru(0001) surface with C₆₀ coverages in the range 0.04–0.4 ML shows the successive occupation of sites within the moiré superlattice (**Figure 3**): *hcp* valley sites are populated first with individual molecules, and then with six additional close-packed molecules, then *fcc* valley sites are filled, then moiré hill sites, and finally six additional close-packed molecules are arranged around the hill sites.^[65] Although the C₆₀ molecules in the *hcp* valley sites rotate when they are

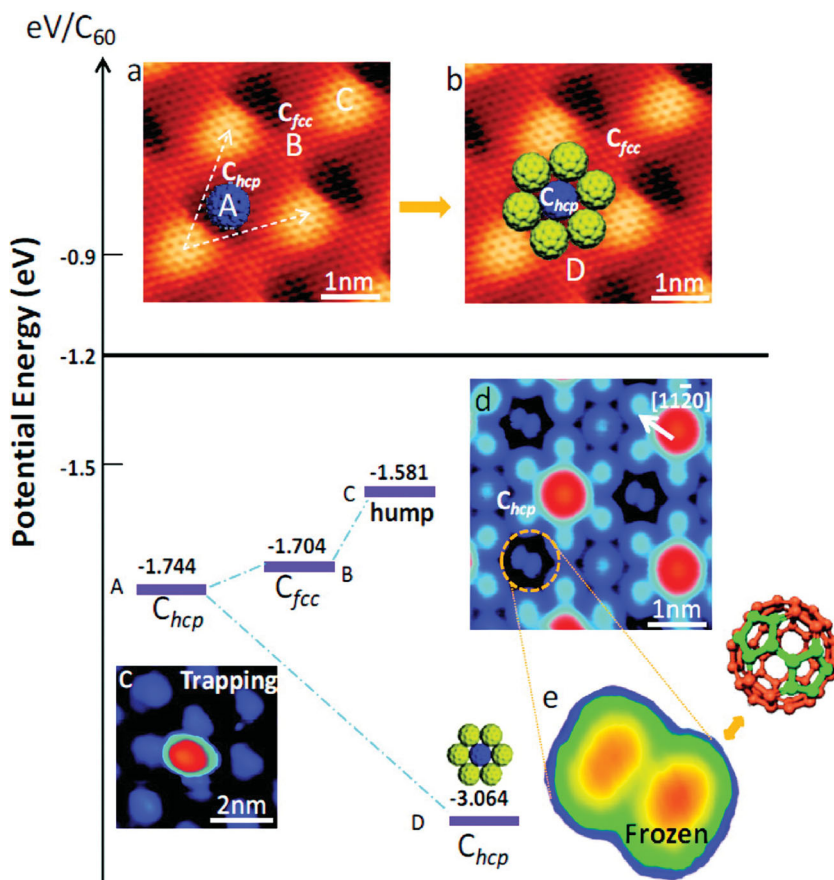


Figure 3. Hierarchical occupation of sites by C₆₀ on graphene/Ru(0001) at room temperature. (a) and (b) schematically show the initially-occupied sites: at low coverage, the C₆₀ first occupies *hcp* valley sites within the moiré pattern, then forms into hexamers surrounding these molecules. (c) shows an STM image corresponding to the scheme in (a). Once the monolayer is completed, the molecules in the *hcp* sites are frozen into place by a crowding effect, as shown in (d) and (e), with the schematic next to (e) showing the orientation of the frozen molecules, which have their 6:6 bonds facing upwards. Reproduced with permission.^[65] Copyright 2012, American Chemical Society.

isolated, as evidenced by their indistinct appearance in STM images, they adopt a fixed orientation (with their 6:6 C—C bonds up) once surrounded by their six nearest-neighbors, which is attributed to a “crowding effect”; the same effect has been credited with stabilizing other molecules in 2D assemblies at room temperature, e.g., guest coronene molecules in a 2D host/guest architecture.^[66] This successive filling of sites can be correlated with the variation in adsorption energies associated with the different moiré sites, which also manifests in anisotropic diffusion barriers and diffusion-limited growth of multilayers of C₆₀.^[65]

On graphene/SiC(0001), deposition of C₆₀ at RT, with subsequent cooling to 45 K, reveals a close-packed structure that appears to be only weakly coupled to the substrate.^[67] The C₆₀ molecules within the layers exhibit no internal structure (as compared to molecules residing on neighboring SiC, which reveal clear submolecular detail), a number of domain orientations are observed and the HOMO-LUMO gap revealed by STS is much larger (3.5 eV) than the gap observed for C₆₀ on coinage metal surfaces, where it is known to interact more strongly.

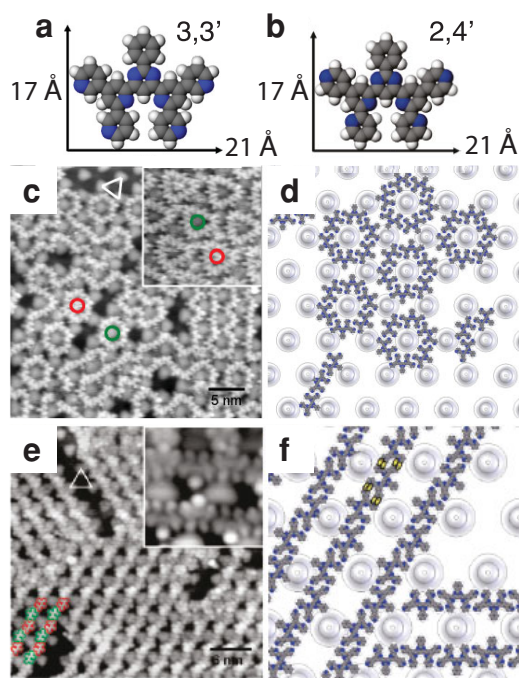


Figure 4. 3,3'-BTP (a) and 2,4'-BTP (b) on graphene/Ru(0001). The 3,3'-BTP forms into a variety of structures on graphene/Ru(0001) (c) avoiding hill sites in the moiré superlattice (d). 2,4'-BTP forms preferentially into linear structures (e) that lie between the moiré hill sites. (a,c,d) Reproduced according to the Creative Commons license.^[50] (b,e,f) Reproduced with permission.^[69] Copyright 2011, American Chemical Society.

4. Exploring Graphene-Based Molecular Assemblies Through Other Molecules

4.1. Studies of Self-Assembly at the Molecular Level

Although the majority of studies thus far have been devoted to PTCDA, phthalocyanines and C_{60} , a growing number of other molecules have also been investigated, creating a broader picture of molecular self-assembly on graphene. These studies reinforce the basic tenets that can be extracted from the previously-described work: the graphene substrate asserts itself most strongly (i) at low temperatures, and (ii) when it has a pronounced moiré pattern, such as epitaxial graphene on Ru(0001). At room temperature on graphene without a pronounced moiré pattern, molecular self-assembly essentially proceeds as it does on HOPG.

The polycyclic aromatics 3,3'- (Figure 4a) and 2,4'- (Figure 4b) bis(terpyridine) (BTP) are designed to form intermolecular C-H...N hydrogen bonds, calculated to have a typical strength of 100 meV.^[68] The 3,3'-positioned nitrogen atoms allow for the formation of chains comprising antiparallel constituents, or for the possibility of curved structures formed from molecules aligned at 60° to one another. Deposition onto graphene/Ru(0001) reveals that 3,3'-BTP forms into a number of geometries, including triangles and circular hexamers surrounding moiré hill sites, and linear chains that run along moiré valleys, without any long-range order

(Figure 5c).^[50] These motifs are similar to the ones exhibited by 3,3'-BTP on HOPG,^[68] but are clearly constrained by the adsorption landscape of the graphene moiré superlattice, which the authors estimate to vary between -0.625 and -0.985 eV between valley and hill sites according to force field calculations.

The 2,4'-positioned nitrogen atoms in 2,4'-BTP are optimized for the formation of linear chains with antiparallel constituents. Following the deposition of multilayers of 2,4'-BTP onto the graphene/Ru(0001) surface, controlled desorption of excess molecules and cooling to temperatures between 115 and 130 K, STM images reveal ordered hydrogen-bonded 1D chains of 2,4'-BTP that selectively run between the hill sites of the moiré superlattice (Figure 4e).^[69] Using force field calculations corrected with a dispersive force, the authors calculate that the hill sites present an adsorption energy 0.63 eV weaker than the energy of a valley site (-3.45 eV vs. -4.08 eV), consistent with the selective adsorption of the 2,4'-BTP chains along moiré valleys.

The same type of hydrogen bonding drives the self-assembly of perylene tetracarboxylic diimide (PTCDI). PTCDI is structurally similar to PTCDA, but with imide groups at the ends of the molecule that allow for C-H...N intermolecular interactions; the functionalized derivatives 1,7-dipropylthio-perylene-3,4:9,10-tetracarboxydiimide (DP-PTCDI) and 1,7-di(butyl)-coronene-3,4:9,10-tetracarboxylic acid bisimide (DB-CTCDI) additionally have alkyl chains at their beltlines. RT STM of PTCDI deposited onto graphene/Rh(111) reveals the formation of lines of PTCDI, stabilized by hydrogen bonds, that have a minimum spacing of $\sqrt{3}/2$ times the moiré superlattice periodicity of 2.95 nm,^[70] much like the structure formed by 2,4'-BTP on graphene/Ru(0001). The alkyl chains of DP-PTCDI and DB-CTCDI introduce new interactions, allowing the formation of chiral trimeric molecular associations, with DP-PTCDI producing both 1D lines and trimer junctions, and DB-CTCDI forming a honeycomb structure with pores located on moiré hill sites.

The ordering of the 2,4'-BTP and PTCDI chain systems arises as a direct consequence of their hydrogen-bonding geometry. Molecules with lower interaction energies, like pentacene, which has only van der Waals interactions between molecules, have to be coaxied into forming ordered structures. Following RT deposition onto graphene/Ru(0001), at low coverage, LT STM imaging shows that pentacene molecules preferentially adsorb into moiré fcc valley sites,^[63,71] next occupying the hcp valleys at higher coverage, but without exhibiting order.^[71] Short-range and long-range ordered phases can be achieved through careful control of the deposition parameters, with higher substrate temperatures leading to more ordered structures.

The behavior of 7,7',8,8'-tetracyano-*p*-quinodimethane (TCNQ) and 2,3,5,6-tetrafluoro-7,7,8,8-tetracyano-*p*-quinodimethane (F4-TCNQ) on graphene/Ir(111) further illustrates the importance of intermolecular interactions in determining molecular assembly on graphene. Both TCNQ and F4-TCNQ are strong electron acceptors, and hence attractive for hole-doping graphene; F4-TCNQ has previously been demonstrated to *p*-dope graphene through photoemission measurements.^[72] Calculations predict flat-lying

adsorption geometries on graphene and the acceptance of ~ 0.3 and ~ 0.4 electrons, respectively, for TCNQ and F4-TCNQ on isolated graphene.^[73] However, when deposited onto graphene/Ir(111) at RT and subsequently cooled, the two molecules exhibit different behavior that can be attributed to their intermolecular interactions: TCNQ forms a close-packed layer stabilized by electrostatic interactions, whereas F4-TCNQ molecules remain isolated from one another in the valley sites of the moiré superlattice due to electrostatic repulsion.^[74]

In other studies of F4-TCNQ on graphene, the focus has been on the electronic modification introduced by the molecular layer.^[75] On graphene/SiC(0001), ARPES experiments showed that charge transfer to a 0.8 nm thick film of F4-TCNQ was sufficient to neutralize the intrinsic *n*-type doping of monolayer graphene on SiC.^[75b] In this work, the adsorption geometry of the molecules was not directly characterized. However, due to the saturation of charge transfer at 0.8 nm coverage, the authors suggest that the F4-TCNQ is adsorbed in an upright geometry, since the long axis of F4-TCNQ measures 0.8 nm. This study was particularly important because the authors showed the same electronic effects were obtained from both UHV-deposited films (molecular beam epitaxy) and films formed using wet chemistry, where graphene/SiC was dipped in a solution of F4-TCNQ in either chloroform or DMSO.

For linear alkanes, the graphene substrates studied to date lead to assembly identical to that that occurs on HOPG, which has been extensively characterized.^[76] The molecules adsorb with their chains aligned along HOPG high-symmetry directions, and pack tightly onto the surface, maximizing intermolecular van der Waals interactions. Two types of alkenes have been investigated on low-interaction graphene surfaces.

AFM images reveal that both octadecylphosphonic acid (OPA) and tetradecylphosphonic acid (TPA), which comprise phosphonic acid headgroups on linear alkyl chains terminated with methyl groups, self-assemble into ordered 2D crystals after spread-coating onto mono- and multilayer-graphene surfaces prepared by exfoliating graphite onto silicon oxide.^[77] Similarly, 10,12-pentacosadiynoic acid, which has been shown to self-assemble on HOPG, behaves essentially the same on graphene/SiC(0001) in UHV.^[78] On HOPG, the molecular adsorption forces the diacetylene moieties into the required geometry for topochemical polymerization, which can be initiated with a voltage pulse from the STM tip^[79,80] or with UV light, a phenomenon that was duplicated on graphene/SiC(0001) (Figure 5).^[78]

This sort of substrate-invariance of assembly is also observed for the self-assembly of benzene-1,4-dicarboxylic acid (terephthalic acid, TPA) on graphene/Pt(111).^[81] The graphene moiré pattern has no effect on the molecular self-assembly, which defines a 3×4 overlayer stabilized by cyclic dimeric hydrogen-bonding between carboxylic groups that is similar to the structure formed on Ag(111) and Au(111). The polycrystalline graphene surface leads to arbitrary rotations of the TPA overlayer that produces a rich variety of domain boundaries, varying from small angle boundaries to very large angle domains, where hydrogen bonding appears

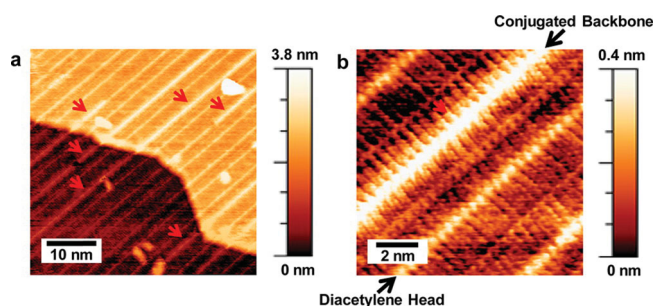


Figure 5. Polymerized films of 10,12-pentacosadiynoic acid on graphene/SiC(0001). (a) STM image obtained after UV photopolymerization of the film, with red arrows denoting polydiacetylene backbones (sample bias 0.7 V). (b) shows a closer view of the conjugated polydiacetylene backbone. Reproduced with permission.^[78] Copyright 2012, American Chemical Society.

to be prioritized over dense molecular packing within the boundary region. The molecular overlayer was observed to extend undisturbed over substrate steps, implying that the graphene continues over the steps and that this perturbation does not perturb the molecular self-assembly.

4.2. Mesoscopic Effects in Molecular Films on Graphene

A study of the polycyclic aromatic para-sexiphenyl (*p*-6P) on graphene provides insight into the self-assembly behavior at the mesoscopic scale. Low energy electron microscopy (LEEM), combined with low energy electron diffraction (LEED), reveals that at temperatures up to 352 K, *p*-6P forms Stranski-Krastanov films on graphene/Ir(111), with both the wetting layer and the needle-like islands preferentially nucleating near wrinkles in the graphene layer.^[82] The quasiepitaxial wetting layer is initially made up of flat-lying molecules, but transforms into a structure comprising one flat-lying and one edge-on molecule per unit cell at a critical coverage; this same structure is found in the 3D islands and is similar to the known structure of the $\{1\bar{1}\bar{1}\}$ surface unit cell for the bulk molecular crystal. On clean Ir(111), *p*-6P forms irregular islands from molecules with their long axes nearly perpendicular to the surface. This study again demonstrates the profound effect of graphene on molecular adsorption geometries and also suggests that non-uniformities in the graphene could also have important effects on the initial stages of molecular film growth; the formation of wrinkles can be a pervasive feature of epitaxial graphene depending on the synthesis route.^[83]

4.3. Covalently-Linked Molecular Structures

Molecular adsorption on graphene has also been used to seed the growth of 2D covalent organic frameworks (COFs), leading to the formation of oriented, aligned multilayer films.^[24b] Three different COFs were formed by condensation using a solvothermal method. In the absence of graphene, the reactions produced insoluble, and hence unprocessable, powders. However, when graphene, supported on either copper,

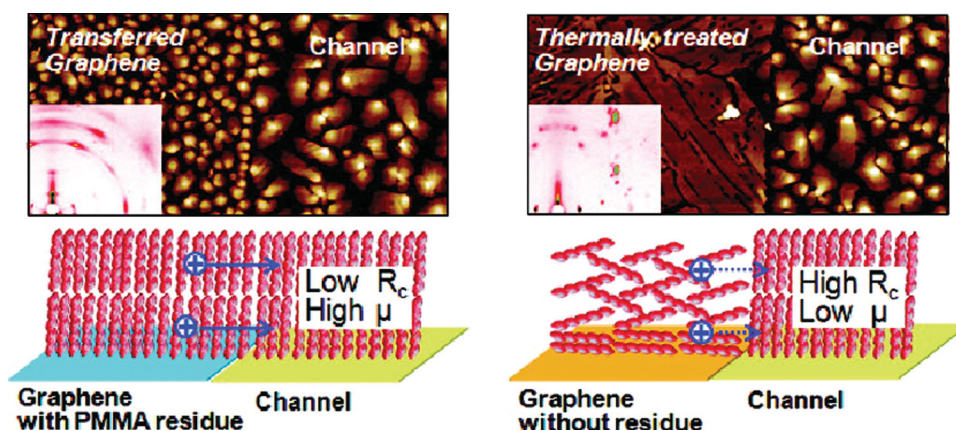


Figure 6. Pentacene growth on polymer-covered (a,c) and clean (b,d) graphene electrodes in a field effect transistor geometry. On the polymer-covered electrode, the pentacene stands upright (c), similar to in the channel region, resulting in a similar morphology as seen in atomic force micrographs (a), and allowing for good lateral charge transport. Conversely, on the clean graphene electrode, the pentacene molecules adsorb flat for the first layers (d), resulting in a much different morphology than the channel region (b) and impeding lateral charge transport. Reproduced with permission.^[88] Copyright 2011, American Chemical Society.

silicon carbide or SiO₂, was introduced to the reaction vessel, multilayer COF films also formed on the graphene. The graphene-supported films were demonstrated by synchrotron x-ray diffraction to be oriented, with the plane of the 2D COF parallel to the plane of the graphene, thus indicating that the presence of graphene facilitated controlled synthesis of the COFs.

This work links conceptually to the emerging field of surface-confined polymerization, where molecular monomers are reacted *in situ* on a suitable substrate to produce monolayer polymer films.^[84] This approach has the potential advantage of allowing for long conjugation lengths in conjugated polymer systems, with the ultimate goal of creating a chemically customizable graphene-like 2D layer. Although the substrates used to date have, in general, been single-crystal metals, similar methodologies could presumably be extended to graphene in order to capitalize on some of its advantageous characteristics.

5. Emerging Applications of Graphene-Supported Molecular Layers

A number of studies have begun to bridge the gap between fundamental explorations of molecular self-assembly on graphene and its application in devices. The controlled growth of molecular films is critical for device applications.^[85] In small molecule devices, maximizing molecular ordering minimizes the charge trapping and scattering associated with defects and disorder.^[86] Furthermore, charge transport in molecular semiconductors is strongly anisotropic,^[87] so the molecular orientation must be consistent with the direction of current flow dictated by the geometry of the device. Carrier mobility in small molecule devices depends on the π -overlap between stacked molecules, and is directed along the stacking axis. Incorporating graphene into device architectures could be very useful in this regard, since even a single layer of graphene appears to facilitate molecular adsorption in predictable geometries.

The previously-described work by Mao et al. is an example of this: using a transferred graphene film, and therefore bypassing the need for high-temperature *in situ* graphene growth, they were able to control the orientation of AlClPc on graphene/ITO, effectively dictating the direction of carrier transport.^[61] Another study exploited the fact that polymer (polymethylmethacrylate, PMMA) residue left behind following graphene transfer induces subsequently-deposited pentacene molecules to stand edge-on on graphene; employing this PMMA-coated graphene as an electrode in a field effect transistor allowed for the fabrication of a device with pentacene oriented in a similar manner on both the electrode and in the channel region (**Figure 6**).^[88] A similar device with the polymer residue removed from the graphene promoted face-on adsorption of pentacene on the electrode (Figure 7) and the corresponding disruption to lateral charge transport at the interface with the channel region led to a significantly lower field-effect mobility (0.4 cm²/V s vs. 1.2 cm²/V s for the polymer-covered electrode.)

Molecular growth on graphene could also be useful in other device-oriented applications. Hersam's group demonstrated the feasibility of selective removal of small regions of PTCDA using feedback controlled lithography; these regions can subsequently be filled with another type of molecule, suggesting a route towards the controlled fabrication of spatially-defined bicomponent films.^[89] The same group also demonstrated that PTCDA layers on graphene have a smoothing effect on the subsequent growth of inorganic materials, including high-*k* dielectrics HfO₂ and Al₂O₃, which grow in rough films on graphene in the absence of a PTCDA layer,^[90] suggesting that molecular self-assembly on graphene may also be a useful tool for optimizing inorganic devices.

6. Conclusions and Outlook

The body of literature generated to date demonstrates that graphene is an amenable substrate for molecular

self-assembly that can impart novel characteristics to overlying molecular structures. The self-assembling systems studied have largely comprised relatively weak intermolecular interactions that have allowed for the clear assertion of substrate effects. On Ru(0001) in particular, epitaxial graphene presents a molecular adsorption energy landscape with substantial periodic variation. Even at RT, the difference in adsorption energies (and concomitant diffusion barriers) between sites within the moiré superlattice is large enough to drive preferential molecular diffusion and adsorption, resulting in templated growth of supramolecular structures and even to the immobilization of certain C₆₀ molecules within a continuous film. On substrates like Ir(111), which imparts a less-pronounced moiré superlattice to epitaxial graphene, LT studies reveal the same type of substrate-driven templating for repulsively interacting molecules.

Conversely, on substrates on which graphene grows with an almost-flat HOPG-like character, molecules behave essentially identically to the way they do on HOPG. The same behaviour appears to extend to non-epitaxial graphene. This increases the versatility of graphene-based self-assembly tremendously, since it removes the requirement for growing graphene directly on the target surface. One of the broad questions to be addressed in graphene-based molecular self-assembly pertains to this point: can transferred or drop-cast graphene be used to facilitate identical molecular self-assembly regardless of the underlying surface? Already there is evidence to support this idea: molecular assembly has been observed to progress on graphene that traverses substrate step edges, or that rests on a nanoscopically rough surface like ITO, suggesting that the graphene may be relatively insensitive to topographic imperfections in the underlying substrate. Presumably, the existence of strong interactions between the overlying molecules and the substrate supporting the graphene may affect the assembly, but this effect remains to be investigated.

The exploration of molecular self-assembly on graphene has only just begun. There are open opportunities to investigate two-dimensional lattices stabilized by metal-organic coordination, opening up possibilities for spin engineering at the graphene surface, and to further explore the possibilities for forming COFs, including monolayer polymers, on graphene. Hierarchical energetics, such as those found in a self-assembled host-guest network could exhibit interesting perturbations if the moiré superlattice could be used to define a superlattice of different types of guest molecules by the variation in adsorption energies. The use of solution-based methods for molecular deposition onto graphene is poised for massive growth, since initial results on F4-TCNQ have indicated consistency between vacuum and solution deposition.^[75b] This approach has the advantage of being rapid and scalable, and can build on the considerable knowledge already accumulated regarding self-assembled molecular layers on HOPG.

Building on rapid progress in the last half-decade, a range of possible fundamental and applications-driven investigations remain to be conducted on graphene, which has emerged as a versatile substrate for molecular self-assembly.

Acknowledgements

This work was supported by the Natural Sciences and Engineering Research Council of Canada (NSERC) through a Discovery Grant, the Fonds Quebecois sur la Recherche en Nature et Technologies (FQRNT) through Team Grants and the Ministère du Développement Économique de l'Innovation et de l'Exportation (MDEIE) through an international collaboration Grant. Federico Rosei is grateful to the Canada Research Chairs program for partial salary support and to the Alexander von Humboldt Foundation for a FW Bessel Award. We thank Dr. J. Lipton-Duffin for his help with the TOC graphic.

- [1] a) K. Novoselov, A. Geim, S. Morozov, D. Jiang, Y. Zhang, S. Dubonos, I. Grigorieva, A. Firsov, *Science* **2004**, *306*, 666–669; b) C. Kane, E. Mele, *Phys. Rev. Lett.* **2005**, *95*, 226801; c) K. Novoselov, A. K. Geim, S. Morozov, D. Jiang, M. K. I. Grigorieva, S. Dubonos, A. Firsov, *Nature* **2005**, *438*, 197–200; d) A. C. Neto, F. Guinea, N. Peres, K. Novoselov, A. Geim, *Rev. Mod. Phys.* **2009**, *81*, 109.
- [2] a) J. Vaari, J. Lahtinen, P. Hautajärvi, *Catal. Lett.* **1997**, *44*, 43–49; b) R. Rosei, M. De Crescenzi, F. Sette, C. Quaresima, A. Savoia, P. Perfetti, *Phys. Rev. B* **1983**, *28*, 1161; c) R. Rosei, S. Modesti, F. Sette, C. Quaresima, A. Savoia, P. Perfetti, *Phys. Rev. B* **1984**, *29*, 3416.
- [3] E. Rollings, G. H. Gweon, S. Y. Zhou, B. S. Mun, J. L. McChesney, B. S. Hussain, A. V. Fedorov, P. N. First, W. A. de Heer, A. Lanzara, *J. Phys. Chem. Sol.* **2006**, *67*, 2172–2177.
- [4] C. Berger, Z. Song, X. Li, X. Wu, N. Brown, C. Naud, D. Mayou, T. Li, J. Hass, A. N. Marchenkov, *Science* **2006**, *312*, 1191–1196.
- [5] Y. S. Dedkov, A. M. Shikin, V. K. Adamchuk, S. L. Molodtsov, C. Laubschat, A. Bauer, G. Kaindl, *Phys. Rev. B* **2001**, *64*, 035405.
- [6] L. Gao, J. R. Guest, N. P. Guisinger, *Nano Lett.* **2010**, *10*, 3512–3516.
- [7] P. W. Sutter, J.-I. Flege, E. A. Sutter, *Nat. Mater.* **2008**, *7*, 406–411.
- [8] S.-Y. Kwon, C. V. Ciobanu, V. Petrova, V. B. Shenoy, J. Bareño, V. Gambin, I. Petrov, S. Kodambaka, *Nano Lett.* **2009**, *9*, 3985.
- [9] J. Coraux, Alpha T. N'Diaye, C. Busse, T. Michely, *Nano Lett.* **2008**, *8*, 565–570.
- [10] P. Sutter, J. T. Sadowski, E. Sutter, *Phys. Rev. B* **2009**, *80*, 245411.
- [11] X. Li, C. W. Magnuson, A. Venugopal, R. M. Tromp, J. B. Hannon, E. M. Vogel, L. Colombo, R. S. Ruoff, *J. Am. Chem. Soc.* **2011**, *133*, 2816.
- [12] G. Ruan, Z. Sun, Z. Peng, J. M. Tour, *ACS nano* **2011**, *5*, 7601–7607.
- [13] V. C. Vincent, C. Tung, M. J. Matthew, J. Allen, Y. Yang Yang, R. B. Richard, B. Kaner (2009) High-throughput solution processing of large-scale graphene. *Nat. Nanotechnol.*, *4*(1), 25–9 [PubMed]
- [14] J. Jinsung Kwak, J. H. Jae Hwan Chu, J. K. Jae-Kyung Choi, S. D. Soon-Dong Park, H. Heungseok Go, S. Y. Sung Youb Kim, K. Kibog Park, S. D. Sung-Dae Kim, Y. W. Young-Woon Kim, E. Euijoon Yoon, S. Suneel Kodambaka, S. Y. Soon-Yong Kwon (2012) Near room-temperature synthesis of transfer-free graphene films. *Nat. Commun.* *3*, 645 [PubMed]
- [15] a) D. V. Kosynkin, A. L. Higginbotham, A. Sinitskii, J. R. Lomeda, A. Dimiev, B. K. Price, J. M. Tour, *Nature* **2009**, *458*, 872–876; b) L. Jiao, L. Zhang, X. Wang, G. Diankov, H. Dai, *Nature* **2009**, *458*, 877–880.
- [16] X. Li, W. Cai, J. An, S. Kim, J. Nah, D. Yang, R. Piner, A. Velamakanni, I. Jung, E. Tutuc, *Science* **2009**, *324*, 1312–1314.

- [17] K. V. Emtsev, A. Bostwick, K. Horn, J. Jobst, G. L. Kellogg, L. Ley, J. L. McChesney, T. Ohta, S. A. Reshanov, J. Röhl, *Nature Mater.* **2009**, *8*, 203–207.
- [18] F. Schwierz, *Nat. Nanotechnol.* **2010**, *5*, 487–496.
- [19] F. Varchon, R. Feng, J. Hass, X. Li, B. N. Nguyen, C. Naud, P. Mallet, J.-Y. Veuille, C. Berger, E. H. Conrad, L. Magaud (2007) Electronic structure of epitaxial graphene layers on SiC: effect of the substrate. *Phys. Rev. Lett.* **99**(12), 126805 [PubMed]
- [20] V. Georgakilas, M. Otyepka, A. B. Bourlinos, V. Chandra, N. Kim, K. C. Kemp, P. Hobza, R. Zboril, K. S. Kim, *Chem. Rev.* **2012**, *112*, 6156–6214.
- [21] A. K. Geim (2009) Graphene: status and prospects. *Science (New York, N.Y.)* **324**(5934), 1530–4 [PubMed]
- [22] a) S. Y. Davydov, *Semiconductors* **2011**, *45*, 618–622; b) T. Hu, I. C. Gerber, *J. Phys. Chem. C* **2013**, *117*, 2411–2420.
- [23] a) M. Batzill, *Surf. Sci. Rep.* **2012**, *67*, 83–115; b) Z. Zhang, H. Huang, X. Yang, L. Zang, *J. Phys. Chem. Lett.* **2011**, *2*, 2897–2905; c) X. Dong, D. Fu, W. Fang, Y. Shi, P. Chen, L. J. Li, *Small* **2009**, *5*, 1422–1426.
- [24] a) J. V. Barth, *Surf. Sci.* **2009**, *603*, 1533–1541; b) J. W. Colson, A. R. Woll, A. Mukherjee, M. P. Levendorf, E. L. Spitler, V. B. Shields, M. G. Spencer, J. Park, W. R. Dichtel, *Science* **2011**, *332*, 228–231; c) A. Langner, S. L. Tait, N. Lin, R. Chandrasekar, V. Meded, K. Fink, M. Ruben, K. Kern, *Angew. Chem. Int. Ed.* **2012**, *124*, 4403–4407.
- [25] O. Ivasenko, D. F. Perepichka, *Chem. Soc. Rev.* **2011**, *40*, 191–206.
- [26] S. De Feyter, F. C. De Schryver, *Chem. Soc. Rev.* **2003**, *32*, 139–150.
- [27] a) R. Gutzler, O. Ivasenko, C. Fu, J. L. Brusso, F. Rosei, D. F. Perepichka, *Chem. Commun.* **2011**, *47*, 9453–9455; b) R. Gutzler, C. Fu, A. Dadvand, Y. Hua, J. M. MacLeod, F. Rosei, D. F. Perepichka, *Nanoscale* **2012**, *4*, 5965–5971.
- [28] S. Yin, C. Wang, X. Qiu, B. Xu, C. Bai, *Surf. Interface Anal.* **2001**, *32*, 248–252.
- [29] Y. Yang, C. Wang, *Chem. Soc. Rev.* **2009**, *38*, 2576–2589.
- [30] M. Surin, P. Samori, *Small* **2007**, *3*, 190–194.
- [31] a) S. Stepanow, M. Lingenfelder, A. Dmitriev, H. Spillmann, E. Delvigne, N. Lin, X. Deng, C. Cai, J. V. Barth, K. Kern, *Nature Mater.* **2004**, *3*, 229–233; b) T. Kudernac, S. Lei, J. A. Elemans, S. De Feyter, *Chem. Soc. Rev.* **2009**, *38*, 402–421.
- [32] a) J. V. Barth, G. Costantini, K. Kern, *Nature* **2005**, *437*, 671–679; b) F. Rosei, M. Schunack, Y. Naitoh, P. Jiang, A. Gourdon, E. Laegsgaard, I. Stensgaard, C. Joachim, F. Besenbacher, *Prog. Surf. Sci.* **2003**, *71*, 95–146; c) F. Rosei, *J. Phys.: Cond. Mat.* **2004**, *16*, S1373; d) F. Ciciora, C. Santato, F. Rosei, in *STM and AFM Studies on (Bio) molecular Systems: Unravelling the Nanoworld*, Springer Berlin Heidelberg, **2008**, pp. 203–267; e) R. Otero, J. M. Gallego, A. L. V. de Parga, N. Martín, R. Miranda, *Adv. Mater.* **2011**, *23*, 5148–5176.
- [33] A. Rochefort, J. D. Wuest, *Langmuir* **2008**, *25*, 210–215.
- [34] a) A. AlZahrani, *Appl. Surf. Sci.* **2010**, *257*, 807–810; b) Y.-H. Zhang, K.-G. Zhou, K.-F. Xie, J. Zeng, H.-L. Zhang, Y. Peng, *Nanotechnology* **2010**, *21*, 065201; c) S. M. Kozlov, F. Viñes, A. Görling, *Carbon* **2012**, *50*, 2482–2492.
- [35] a) S. Zhou, G.-H. Gweon, A. Fedorov, P. First, W. De Heer, D.-H. Lee, F. Guinea, A. C. Neto, A. Lanzara, *Nat. Mater.* **2007**, *6*, 770–775; b) Y. Pan, H. Zhang, D. Shi, J. Sun, S. Du, F. Liu, H. j. Gao, *Adv. Mater.* **2009**, *21*, 2777–2780.
- [36] a) J. Winterlin, M. L. Bocquet, *Surf. Sci.* **2009**, *603*, 1841–1852; b) We note that there is some ambiguity of the naming of these moiré sites in the literature, since some authors refer to the sites by the alignment of the graphene hexagon centres, rather than by the alignment of the carbon atoms, which reverses the fcc/hcp site naming. However, where we refer to these sites in this Review, they are named in terms of the alignment of carbon atoms, and are consistent with the notation used in the papers we describe.
- [37] M. Kralj, I. Pletikosić, M. Petrović, P. Pervan, M. Milun, C. Busse, T. Michely, J. Fujii, I. Vobornik, *Phys. Rev. B* **2011**, *84*, 075427.
- [38] A. T. N'Diaye, S. Bleikamp, P. J. Feibelman, T. Michely, *Phys. Rev. Lett.* **2006**, *97*, 215501.
- [39] a) Y. Pan, M. Gao, L. Huang, F. Liu, H.-J. Gao, *Appl. Phys. Lett.* **2009**, *95*, 093106–093106–093103; b) K. Donner, P. Jakob, *J. Chem. Phys.* **2009**, *131*, 164701.
- [40] A. J. Martínez-Galera, J. M. Gómez-Rodríguez, *J. Phys. Chem. C* **2011**, *115*, 23036–23042.
- [41] R. Erni, M. D. Rossell, M.-T. Nguyen, S. Blankenburg, D. Passerone, P. Hartel, N. Alem, K. Erickson, W. Gannett, A. Zettl, *Phys. Rev. B* **2010**, *82*, 165443.
- [42] P. Lauffer, K. V. Emtsev, R. Graupner, T. Seyller, L. Ley, *Phys. Status Solidi b* **2008**, *245*, 2064–2067.
- [43] C. Ludwig, B. Gompf, W. Glatz, J. Petersen, W. Eisenmenger, M. Möbus, U. Zimmermann, N. Karl, *Z. Phys. B – Cond. Mat.* **1992**, *86*, 397–404.
- [44] S. R. Forrest, *Chem. Rev.* **1997**, *97*, 1793–1896.
- [45] a) T. Schmitz-Hübsch, T. Fritz, F. Sellam, R. Staub, K. Leo, *Phys. Rev. B* **1997**, *55*, 7972–7976; b) K. Glöckler, C. Seidel, A. Soukopp, M. Sokolowski, E. Umbach, M. Böhlinger, R. Berndt, W. D. Schneider, *Surf. Sci.* **1998**, *405*, 1–20; c) T. Wagner, A. Bannani, C. Bobisch, H. Karacuban, R. Möller, *J. Phys.: Cond. Mat.* **2007**, *19*, 056009.
- [46] Q. H. Wang, M. C. Hersam, *Nat. Chem.* **2009**, *1*, 206–211.
- [47] X. Tian, J. Xu, X. Wang, *J. Phys. Chem. C* **2010**, *114*, 20917–20924.
- [48] H. Huang, S. Chen, X. Gao, W. Chen, A. T. S. Wee, *ACS Nano* **2009**, *3*, 3431–3436.
- [49] M. Meissner, M. Gruenewald, F. Sojka, C. Udhardt, R. Forker, T. Fritz, *Surf. Sci.* **2012**, *606*, 1709–1715.
- [50] M. Roos, B. Uhl, D. Künzel, H. E. Hoster, A. Groß, R. J. Behm, *Beilstein J. Nanotechnol.* **2011**, *2*, 365.
- [51] J. D. Emery, Q. H. Wang, M. Zarrouati, P. Fenter, M. C. Hersam, M. J. Bedzyk, *Surf. Sci.* **2011**, *605*, 1685–1693.
- [52] M. Mura, X. Sun, F. Silly, H. T. Jonkman, G. A. D. Briggs, M. R. Castell, L. N. Kantorovich, *Phys. Rev. B* **2010**, *81*, 195412.
- [53] a) K. Walzer, M. Hietschold, *Surf. Sci.* **2001**, *471*, 1–10; b) W. Dou, S. Huang, R. Zhang, C. Lee, *J. Chem. Phys.* **2011**, *134*, 094705.
- [54] J. Mao, H. Zhang, Y. Jiang, Y. Pan, M. Gao, W. Xiao, H.-J. Gao, *J. Am. Chem. Soc.* **2009**, *131*, 14136–14137.
- [55] H. Zhang, J. Sun, T. Low, L. Zhang, Y. Pan, Q. Liu, J. Mao, H. Zhou, H. Guo, S. Du, *Phys. Rev. B* **2011**, *84*, 245436.
- [56] K. Yang, W. Xiao, Y. Jiang, H. Zhang, L. Liu, J. Mao, H. Zhou, S. Du, H.-J. Gao, *J. Phys. Chem. C* **2012**, *116*, 14052–14056.
- [57] Y.-L. Wang, J. Ren, C.-L. Song, Y.-P. Jiang, L.-L. Wang, K. He, X. Chen, J.-F. Jia, S. Meng, E. Kaxiras, *Phys. Rev. B* **2010**, *82*, 245420.
- [58] a) M. Scardamaglia, G. Forte, S. Lizzit, A. Baraldi, P. Lacovig, R. Larciprete, C. Mariani, M. G. Betti, *J. Nanopart. Res.* **2011**, *13*, 6013–6020; b) M. Scardamaglia, S. Lisi, S. Lizzit, A. Baraldi, R. Larciprete, C. Mariani, M. G. Betti, *J. Phys. Chem. C* **2013**, *117*, 3019–3027.
- [59] S. K. Hämäläinen, M. Morozova, R. Drost, P. Liljeroth, J. Lahtinen, J. Sainio, *J. Phys. Chem. C* **2012**, *116*, 20433–20437.
- [60] W. Dou, S. Huang, R. Q. Zhang, C. S. Lee, (2011) Molecule-substrate interaction channels of metal-phthalocyanines on graphene on Ni(111) surface. *The Journal of chemical physics* **134**(9) 094705 [PubMed]
- [61] H. Y. Mao, R. Wang, Y. Wang, T. Chao Niu, J. Q. Zhong, M. Yang Huang, D. Chen Qi, K. Ping Loh, A. Thyne Shen Wee, W. Chen, *Appl. Phys. Lett.* **2011**, *99*, 093301.
- [62] K. Xiao, W. Deng, J. K. Keum, M. Yoon, I. V. Vlasiouk, K. W. Clark, A.-P. Li, I. I. Kravchenko, G. Gu, E. A. Payzant, *J. Am. Chem. Soc.* **2013**, *135*, 3680–3687.
- [63] H. Zhou, J. Mao, G. Li, Y. Wang, X. Feng, S. Du, K. Mullen, H.-J. Gao, *Appl. Phys. Lett.* **2011**, *99*, 153101–153101–153103.

- [64] G. Li, H. Zhou, L. Pan, Y. Zhang, J. Mao, Q. Zou, H. Guo, Y. Wang, S. Du, H.-J. Gao, *Appl. Phys. Lett.* **2012**, *100*, 013304.
- [65] J. Lu, P. S. E. Yeo, Y. Zheng, Z. Yang, Q. Bao, C. K. Gan, K. P. Loh, *ACS Nano* **2012**, *6*, 944–950.
- [66] J. M. MacLeod, Z. Ben Chaouch, D. Perepichka, F. Rosei, *Langmuir* **2013**, *29*, 7318–7324.
- [67] J. Cho, J. Smerdon, L. Gao, Ö. Süzer, J. R. Guest, N. P. Guisinger, *Nano Lett.* **2012**, *12*, 3018–3024.
- [68] C. Meier, M. Roos, D. Künzel, A. Breitruck, H. E. Hoster, K. Landfester, A. Gross, R. J. r. Behm, U. Ziener, *J. Phys. Chem. C* **2009**, *114*, 1268–1277.
- [69] M. Roos, D. Künzel, B. Uhl, H.-H. Huang, O. Brandao Alves, H. E. Hoster, A. Gross, R. J. r. Behm, *J. Am. Chem. Soc.* **2011**, *133*, 9208–9211.
- [70] A. J. Pollard, E. W. Perkins, N. A. Smith, A. Saywell, G. Goretzki, A. G. Phillips, S. P. Argent, H. Sachdev, F. Müller, S. Hüfner, *Angew. Chem. Int. Ed.* **2010**, *49*, 1794–1799.
- [71] H. Zhou, L. Zhang, J. Mao, G. Li, Y. Zhang, Y. Wang, S. Du, W. A. Hofer, H.-J. Gao, *Nano Res.* **2012**, *6*, 131–137.
- [72] W. Chen, S. Chen, D. C. Qi, X. Y. Gao, A. T. S. Wee, *J. Am. Chem. Soc.* **2007**, *129*, 10418–10422.
- [73] J. Sun, Y. Lu, W. Chen, Y. Feng, A. Wee, *Phys. Rev. B* **2010**, *81*, 155403.
- [74] S. Barja, M. Garnica, J. J. Hinarejos, A. L. V. de Parga, N. Martín, R. Miranda, *Chem. Commun.* **2010**, *46*, 8198–8200.
- [75] a) X. Wang, J.-B. Xu, W. Xie, J. Du, *J. Phys. Chem. C* **2011**, *115*, 7596–7602; b) C. Coletti, C. Riedl, D. Lee, B. Krauss, L. Patthey, K. Von Klitzing, J. Smet, U. Starke, *Phys. Rev. B* **2010**, *81*, 235401.
- [76] a) J. P. Rabe, S. Buchholz, *Science* **1991**, *253*, 424–427; b) K. G. Nath, O. Ivasenko, J. M. MacLeod, J. A. Miwa, J. D. Wuest, A. Nanci, D. F. Perepichka, F. Rosei, *J. Phys. Chem. C* **2007**, *111*, 16996–17007.
- [77] M. C. Prado, R. Nascimento, L. G. Moura, M. J. Matos, M. S. Mazzoni, L. G. Cancado, H. Chacham, B. R. Neves, *ACS Nano* **2011**, *5*, 394–398.
- [78] A. Deshpande, C.-H. Sham, J. M. Alaboson, J. M. Mullin, G. C. Schatz, M. C. Hersam, *J. Am. Chem. Soc.* **2012**, *134*, 16759–16764.
- [79] Y. Okawa, M. Aono, *J. Chem. Phys.* **2001**, *115*, 2317.
- [80] Y. Okawa, M. Aono, *Nature* **2001**, *409*, 683–684.
- [81] R. Addou, M. Batzill, *Langmuir* **2013**, *29*, 6354–6360.
- [82] a) G. Hlawacek, F. S. Khokhar, R. van Gastel, B. Poelsema, C. Teichert, *Nano Lett.* **2011**, *11*, 333–337; b) F. S. Khokhar, G. Hlawacek, R. Van Gastel, H. J. Zandvliet, C. Teichert, B. Poelsema, *Surf. Sci.* **2011**, *606*, 475–480.
- [83] S. J. Chae, F. Güneş, K. K. Kim, E. S. Kim, G. H. Han, S. M. Kim, H. J. Shin, S. M. Yoon, J. Y. Choi, M. H. Park, *Adv. Mater.* **2009**, *21*, 2328–2333.
- [84] M. El Garah, J. M. MacLeod, F. Rosei, *Surf. Sci.* **2013**, *613*, 6–14.
- [85] W. Shao, H. Dong, L. Jiang, W. Hu, *Chemical Science* **2011**, *2*, 590–600.
- [86] O. D. Jurchescu, J. Baas, T. Palstra, *Appl. Phys. Lett.* **2004**, *84*, 3061–3063.
- [87] V. Coropceanu, J. Cornil, D. A. da Silva Filho, Y. Olivier, R. Silbey, J.-L. Brédas, *Chem. Rev.* **2007**, *107*, 926–952.
- [88] W. H. Lee, J. Park, S. H. Sim, S. Lim, K. S. Kim, B. H. Hong, K. Cho, *J. Am. Chem. Soc.* **2011**, *133*, 4447–4454.
- [89] Q. H. Wang, M. C. Hersam, *Nano Lett.* **2010**, *11*, 589–593.
- [90] a) J. M. Alaboson, Q. H. Wang, J. D. Emery, A. L. Lipson, M. J. Bedzyk, J. W. Elam, M. J. Pellin, M. C. Hersam, *ACS Nano* **2011**, *5*, 5223–5232; b) J. E. Johns, H. J. Karmel, J. M. Alaboson, M. C. Hersam, *J. Phys. Chem. Lett.* **2012**, *3*, 1974–1979.

Received: June 27, 2013
 Published online: October 24, 2013